Geological Society of America
Special Paper 346
2000

Recognition of primary and diagenetic magnetizations to determine the magnetic polarity record and timing of deposition of the moat-fill rocks of the Oligocene Creede caldera, Colorado

Richard L. Reynolds
U.S. Geological Survey, Box 25046, M.S. 980, Denver, Colorado 80225 USA
Joseph G. Rosenbaum
U.S. Geological Survey, Box 25046, M.S. 980, Denver, Colorado 80225 USA
Donald S. Sweetkind
U.S. Geological Survey, Box 25046, M.S. 980, Denver, Colorado 80225 USA
Marvin A. Lanphere
U.S. Geological Survey, M.S. 937, Menlo Park, California 94025 USA
Andrew P. Roberts
Department of Oceanography, University of Southampton, Southampton Oceanography Centre, Southampton SO14 3ZH, United Kingdom
Kenneth L. Verosub
Department of Geology, University of California, Davis, California 95616 USA

ABSTRACT

Sedimentary and volcaniclastic rocks of the Oligocene Creede Formation fill the moat of the Creede caldera, which formed at about 26.9 Ma during the eruption of the Snowshoe Mountain Tuff. Paleomagnetic and rock magnetic studies of two cores (418 and 703 m long) that penetrated the lower half of the Creede Formation, in addition to paleomagnetic and isotopic dating studies of stratigraphically bracketing volcanic units, provide information on the age and the time span of sedimentation of the caldera fill. Normal polarity magnetizations are found in Snowshoe Mountain Tuff beneath the moat sediments; in detrital-magnetite–bearing graded tuffs near the bottom of the moat fill; in an ash-fall deposit about 200 m stratigraphically above the top of core 2; and in postcaldera lava flows of the Fisher Dacite that overlie the Creede Formation. Normal polarity also characterizes detrital-magnetite–bearing tuff and sandstone units within the caldera moat rocks that did not undergo severe sulfidic alteration. The combination of initially low magnitude of remanent magnetization and the destructive effects of subsequent diagenetic sulfidization on detrital iron oxides results in a poor paleomagnetic record for the fine-grained sedimentary rocks of the Creede Formation. These fine-grained rocks have either normal or reversed polarity magnetizations that are carried by magnetite and/or maghemite. Many more apparent reversals are found than can be accommodated by any geomagnetic polarity time scale over the interval spanned by the ages of the bracketing extrusive rocks. Moreover, opposite polarity magnetizations are found in specimens separated by only a few centimeters, without intervening hiatuses, and by specimens in several tuff beds, each of which represents a single depositional event. These polarity changes cannot, therefore, be attributed to detrital remanent mag-

Reynolds, R. L., Rosenbaum, J. G., Sweetkind, D. S., Lanphere, M. A., Roberts, A. P., and Verosub, K. L., 2000, Recognition of primary and diagnetic magnetizations to determine the magnetic polarity record and timing of deposition of the moat-fill rocks of the Oligocene Creede caldera, Colorado, *in* Bethke, P. M., and Hay, R. L., eds., Ancient Lake Creede: Its volcano-tectonic setting, history of sedimentation, and relation to mineralization in the Creede Mining District: Boulder, Colorado, Geological Society of America Special Paper 346.

netization. Many polarity changes are apparently related to chemical remanent magnetizations carried by postdepositional magnetite and maghemite that formed in rocks in which most or all detrital magnetic iron oxide was destroyed. Incipient oxidation of early diagenetic pyrite may have produced the secondary magnetic iron oxides. The $^{40}Ar/^{39}Ar$ dates on the normal polarity Snowshoe Mountain Tuff (26.89 ± 0.05 Ma, 1 σ) and on the normal polarity postcaldera Fisher lava flows (as young as 26.23 ± 0.05 Ma, 1 σ) indicate that deposition of the Creede Formation spanned about 340–660 k.y. The intermittently defined normal polarity magnetization for the caldera-fill sequence, compared with the different versions of the geomagnetic polarity time scale, is consistent with the shorter time span.

INTRODUCTION

Sedimentary and volcaniclastic deposits of the Oligocene Creede Formation that fill the moat of the 26.9 Ma Creede caldera (Lipman, this volume) are the target of multidisciplinary investigations to test theories about the fluid and geochemical links between the moat fill and the Creede mineralized vein system. Paleomagnetic and rock magnetic studies of the Creede Formation in Creede caldera moat cores (Fig. 1) were undertaken primarily to determine the time span represented by the moat fill and to enable correlation between cores. In this chapter, paleomagnetic results are summarized from a variety of moat-fill lacustrine and pyroclastic rocks in the cores that penetrated approximately the lower half of the Creede Formation. The results are supplemented by paleomagnetic data from volcanic rocks that underlie or cap the Creede Formation. An earlier progress report on magnetic properties of the Creede Formation focused on depositional mechanisms of pyroclastic rocks, on relations between rock types and magnetic susceptibility, and on the recognition of postdepositional alteration of the Creede Formation and its possible paleomagnetic complications (Reynolds et al., 1994). The geologic setting and goals of the overall project were summarized by Bethke and Lipman (1987), Campbell (1993), and Bethke (1994). The core material was described by Hulen (1992). In this chapter, we follow the stratigraphic nomenclature of Larsen and Crossey (1996) and Larsen and Nelson (this volume), who discuss the general stratigraphy of the cores and the geophysical properties of the boreholes. The deposits of the Creede Formation are described in detail by Larsen and Crossey (1996; this volume), Finkelstein et al. (this volume), and Heiken and Krier (this volume).

Measured paleomagnetic polarities from the Creede Formation yield a polarity sequence that is geologically and geomagnetically unreasonable. This complex record apparently arises from both depositional remanent magnetization (DRM) and chemical remanent magnetization (CRM), apparently caused by the production of magnetic minerals from pyrite. These results thus have broad relevance for magnetic studies of sedimentary rocks in which postdepositional pyrite is susceptible to oxidation to produce even younger iron oxide minerals. A skeletal polarity record that spans the depositional history of the intracaldera fill was constructed using results from the DRM of a few ash-fall tuff beds and from the thermal remanent magnetization (TRM, or partial PTRM) of unaltered pyroclastic and extrusive rocks that bracket the Creede Formation.

Another complication of the paleomagnetic results from drill core may have arisen from the coring process. Core barrels have an axial magnetic field that may induce an axially directed isothermal remanent magnetization (IRM) to core material. Typically, IRM associated with drilling results in strong NRM (N = natural) magnitudes with near-vertical inclinations that are mostly demagnetized by low alternating fields.

GEOCHRONOLOGIC LIMITS ON THE AGE AND DURATION OF DEPOSITION OF THE CREEDE FORMATION

A magnetic stratigraphy may contain a detailed temporal record of geomagnetic field behavior if the magnetizations were acquired at or very shortly after deposition and in the absence of major depositional hiatuses (e.g., Jacobs, 1984). Such a record must be compatible with available geochronometric data; in this study these are provided by $^{40}Ar/^{39}Ar$ isotopic dates on the Snowshoe Mountain Tuff (Lanphere, this volume), which underlies the Creede Formation, and on lava flows of the Fisher Dacite that erupted after caldera collapse. Reliable ages for the Creede Formation could not be measured directly; total-fusion $^{40}Ar/^{39}Ar$ ages on biotite from five ash layers in the two moat holes yielded inconsistent results, reflecting the presence of reworked material (Lanphere, 1994; this volume). The youngest date obtained from ash beds from the drill core is 26.13 ± 0.19 Ma (Lanphere, this volume).

Lanphere (this volume) obtained a $^{40}Ar/^{39}Ar$ date of 26.92 ± 0.07 Ma for the Snowshoe Mountain Tuff in core 2 and an exposure of outflow tuff. Lanphere (this volume) also determined an age of 26.26 ± 0.04 Ma for Fisher Dacite that represents a pooled estimate of dates from lavas that overlie the Creede Formation on Fisher Mountain and Copper Mountain. Two localities of older Fisher Dacite, which erupted early in the caldera-filling history, have also been dated. The Fisher lava flow at Wagon Wheel Gap yielded $^{40}Ar/^{39}Ar$ laser total fusion and incremental-heating plateau ages on biotite of 26.59 ± 0.09 Ma and 26.68 ± 0.14 Ma, respectively (Lanphere, this volume). The Fisher lava flow near McCall Creek at the west side of the caldera (see Lipman, this vol-

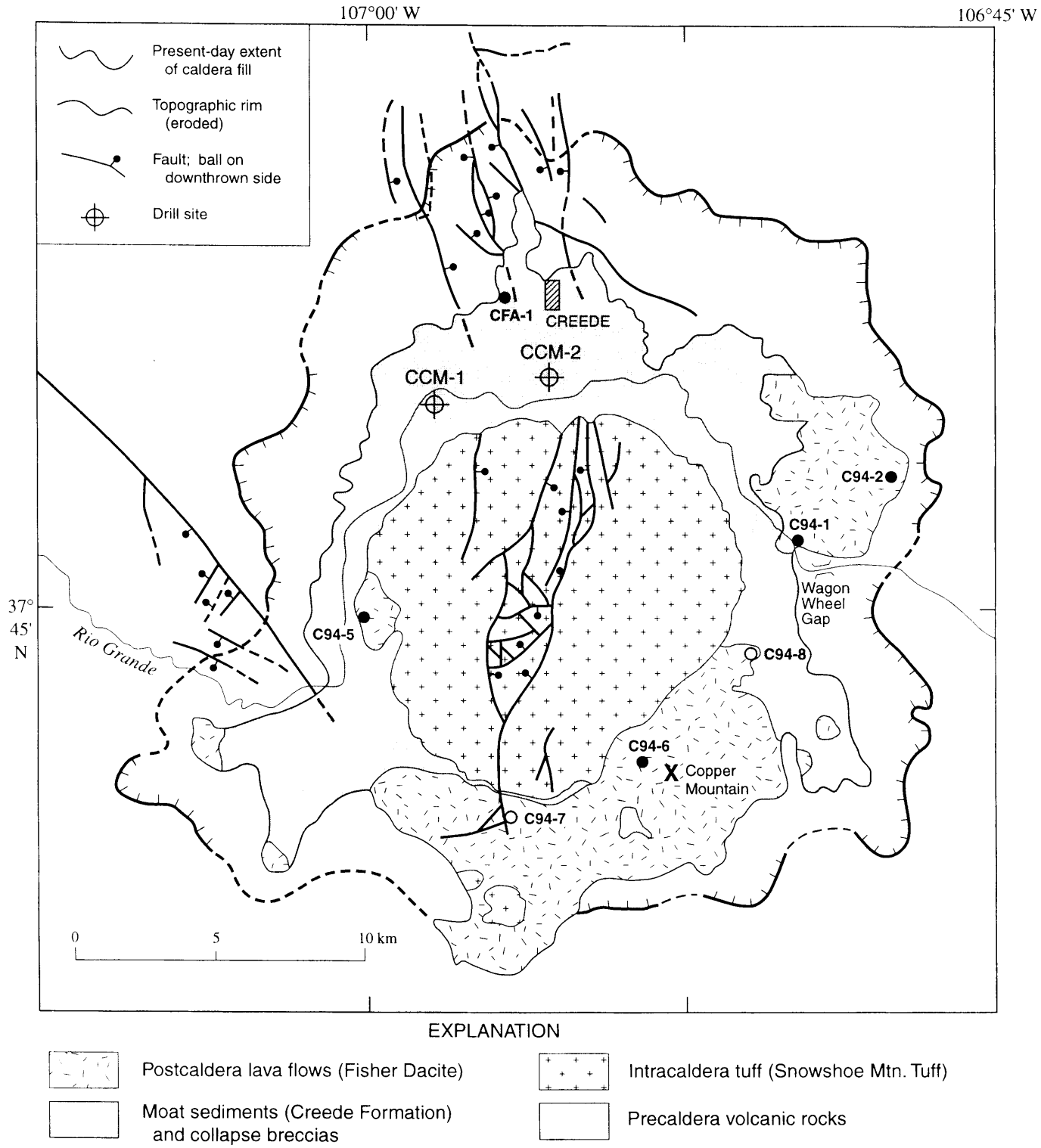

Figure 1. Generalized geologic map of Creede caldera, showing approximate locations of eroded topographic rim; present-day extent of caldera-fill deposits; normal faults related to resurgent doming of Creede caldera and mineralization of Creede district; drill cores 1 and 2 (CCM-1 and CCM-2, respectively); and outcrop sampling sites for Fisher Dacite (C94 sites) and ash-fall tuff (CFA-1 site). Dots indicate sampled outcrops of volcanic rock. Closed symbols indicate that reliable paleomagnetic results were obtained from site, and open symbols indicate unreliable results. See also Figures 14 and 15. Modified from Lipman (this volume).

ume) yielded a $^{40}Ar/^{39}Ar$ date of 26.63 ± 0.09 Ma (Lanphere this volume). The ages were determined using standard biotite (SB-3, K-Ar age of 162.9 ± 1.3 Ma) as the flux monitor, using techniques described by Dalrymple and Lanphere (1971, 1974), Dalrymple et al. (1981), and Lanphere (1988). Considering the isotopic dates, including uncertainties (in this chapter, all isotopic dates are reported at ±1 σ error level) of the bracketing volcanic units, deposition of the Creede Formation probably occurred over a period of about 0.34–0.66 m.y. The 0.66 m.y. period is represented by different patterns in three recent geomagnetic polarity time scales (GPTS): mostly normal polarity but reversed in the upper part (Harland et al., 1990), mostly normal but reversed in the lower part (Wei, 1995), and about evenly divided reversed (lower half) and normal (upper half) polarity (Cande and Kent, 1995; Fig. 2). The Snowshoe Mountain Tuff and three previously sampled flows of the Fisher Dacite have normal polarity magnetizations (Rosenbaum et al., 1987; Tanaka and Kono, 1973; Beck et al., 1977).

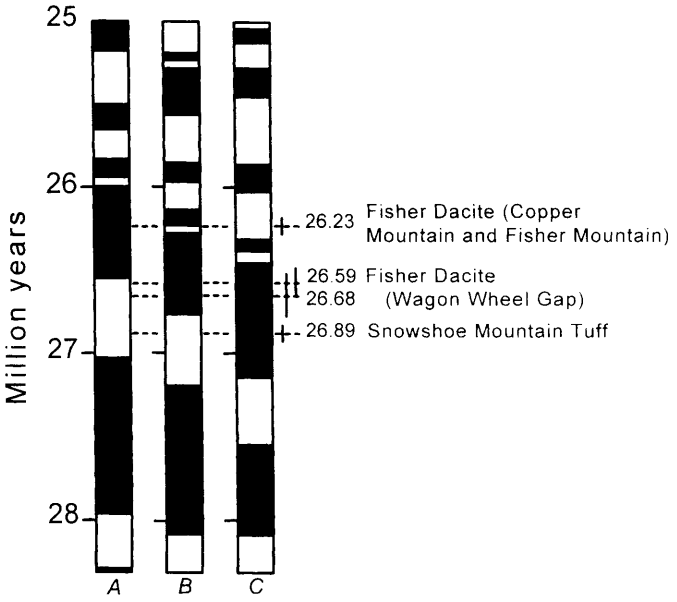

Figure 2. Part of Oligocene geomagnetic polarity time scales (from A, Cande and Kent, 1995; B, Wei, 1995; and C, Harland et al., 1990) with $^{40}Ar/^{39}Ar$ isotopic dates for volcanic units that underlie, are within, and overlie sedimentary rocks of Creede Formation (from Lanphere, this volume). Vertical bars on right side indicate 1 σ analytical uncertainty for each listed date. Filled area indicates normal polarity; open area indicates reversed polarity.

METHODS

Magnetic susceptibility (MS) was measured on whole-core segments and on standard paleomagnetic specimens (volume about 10 cm^3). Measurements were made at 600 Hz in a field of about 0.1 mT using susceptometers that were calibrated using MnO_2 standards. Hysteresis properties of paleomagnetic samples were determined using a vibrating sample magnetometer. Paleomagnetic measurements of samples (5–15 g cylinders) were made using four different magnetometers: two cryogenic magnetometers and two spinner magnetometers. Core samples were oriented vertically but not azimuthally. Directions of remanent magnetization (see Reynolds et al., 1994, Table 1) were determined by least-squares line fitting of demagnetization decay paths on vector diagrams (Zijderveld, 1967; Kirschvink, 1980). Each sample was demagnetized either in progressive alternating fields (AFs), typically in 10 steps from 5 mT to 80 mT, or by thermal techniques, typically in 8 steps from 100 to 600 °C. Demagnetization results provide important information on the identity of magnetic minerals in the remanence decay as a function of peak AF or temperature.

To facilitate analysis and discussion of paleomagnetic results from the cores, we assigned a quality rating to the magnetization decay path for each sample (Fig. 3). The highest rating of 1 was reserved for results in which the demagnetization path decayed toward the origin in a near straight line. A rating of 2 was assigned to paths that were curved or kinked and that trended generally toward the origin but that clearly defined a positive or negative inclination. A quality rating of 3 was assigned to paths that typically have a cluster of points at either inclination sign but without a clear decay to the origin. About 5% of the more than 360 specimens analyzed gave completely erratic results and were eliminated from further analysis.

The magnitude of NRM also factored in the evaluation of the paleomagnetic data. Not surprisingly, the NRM magnitude and quality of the demagnetization path are commonly linked. In the following we refer to magnetizations as either strong (those having NRM magnitude $>10^{-2}$ A/m [10^{-5} emu/cm^3]), moderately strong (NRM magnitude between 2×10^{-3} and 10^{-2} A/m), or weak (NRM $<2 \times 10^{-3}$ A/m). In the following discussion, we make use of the quality rating and NRM magnitude to assess the reliability of the paleomagnetic directions.

Other methods for identifying magnetic minerals include thermomagnetic analysis and direct petrographic observation. Thermomagnetic analysis, the measurement of high-field magnetization as a function of temperature, was used to test for the presence of magnetic iron oxide and iron sulfide minerals which have diagnostic Curie temperatures and/or characteristic shapes of their thermomagnetic curves. Iron oxide and iron sulfide minerals were examined using standard reflected-light microscopy at magnifications to about 500×. We viewed 64 polished thin sections made from paleomagnetic samples and 10 polished mounts of grains that were separated magnetically from bulk samples.

EFFECT OF LITHOLOGIC VARIATION AND DIAGENETIC ALTERATION ON PALEOMAGNETIC RESULTS FROM THE CREEDE FORMATION

Both lithologic zonation and postdepositional alteration exert a strong influence on the rock magnetic properties and, consequently, on the paleomagnetic record of the Creede Formation. The lower part of the Creede Formation dominantly consists of tuff breccia, conglomerate, and fluvial sandstone,

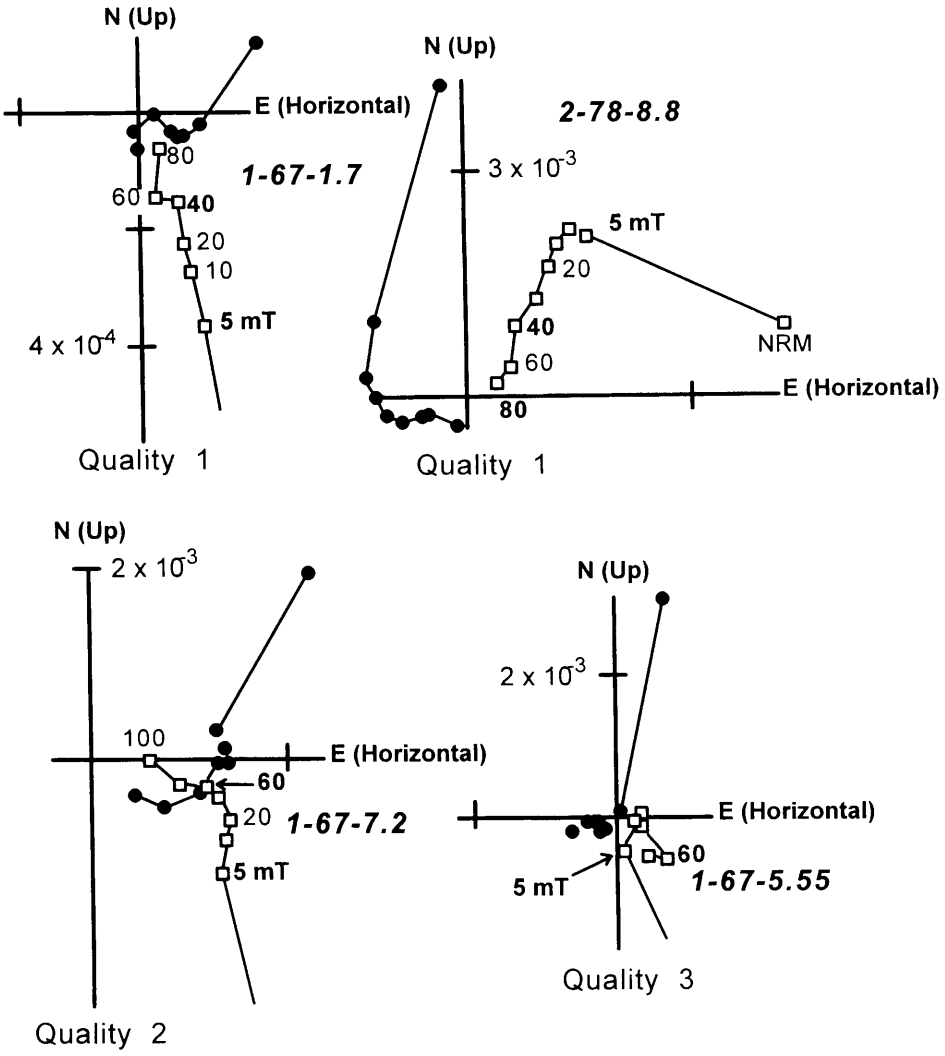

Figure 3. Orthogonal vector diagrams (see Zijderveld, 1967) illustrating three categories of quality of alternating field (AF) demagnetization path, from high (1) to poor (3). Two diagrams illustrate quality 1 result: specimen 1-67-1.7, having normal polarity magnetization, and specimen 2-78-8.8, having reverse polarity magnetization. (Demagnetization steps are in mT). Natural remanent magnetization (NRM) inclination points are off scale in three diagrams illustrating normal polarity. Closed symbols represent projections of magnetic vector onto horizontal plane. Open symbols represent projections of magnetic vector onto vertical plane. (Remanent magnetizations are given in A/m).

representing high-energy, coarse-grained facies. In contrast, the upper part dominantly consists of laminated beds of silty, reworked tuff with intervening ash-fall tuff beds, representing low-energy, fine-grained depositional facies. The coarse-grained beds generally have high NRM magnitude and MS (typically $>10^{-2}$ volume SI; Fig. 4), as expected because of the abundant magnetite in the heavy-mineral laminations of the sandstone as well as in the volcanic-rock clasts of the breccia and conglomerate. The fine-grained beds have much lower NRM magnitude and MS (typically $<2.5 \times 10^{-4}$ volume SI), as would be expected on the basis of lower energies of sediment transport to the lake bottom.

The boundary between the high- and low-MS zones does not exactly coincide with the lithologic boundary between the two facies, but rather is present within the coarse-grained rocks (Fig. 4). This break thus corresponds more closely to a geochemical boundary than to a depositional boundary. In core 1, the MS break occurs between about 305 and 320 m within an interval of interbedded pebble to cobble conglomerate and pebbly sandstone, whereas in core 2 the break occurs between about 505 and 530 m within a thick monomictic breccia.

The geochemical boundary separates a less altered zone containing sparse pyrite in the lower third of the cores from an overlying, more altered upper zone that is characterized by abundant pyrite. The pyrite is a diagenetic product of bacterial sulfate reduction (McKibben et al., 1993; Rye et al., this volume, Chapter 11). Because alteration strongly affected the magnetic properties of much of the Creede Formation, it is important to consider the paleomagnetic results in light of sulfur geochemical data and petrographic observations of sulfidic alteration.

The relations between sulfur content and MS illustrate the effects of sulfidization on magnetic properties (Fig. 5). MS values have a strong inverse relation to total sulfur content regardless of lithology. In this setting, total sulfur is a proxy for iron sulfide minerals because of the absence of sulfate minerals, such as barite or gypsum, in the Creede Formation. Further evidence for iron sulfide came from MS measurements of samples after thermal demagnetization steps. An original presence of iron sulfide in

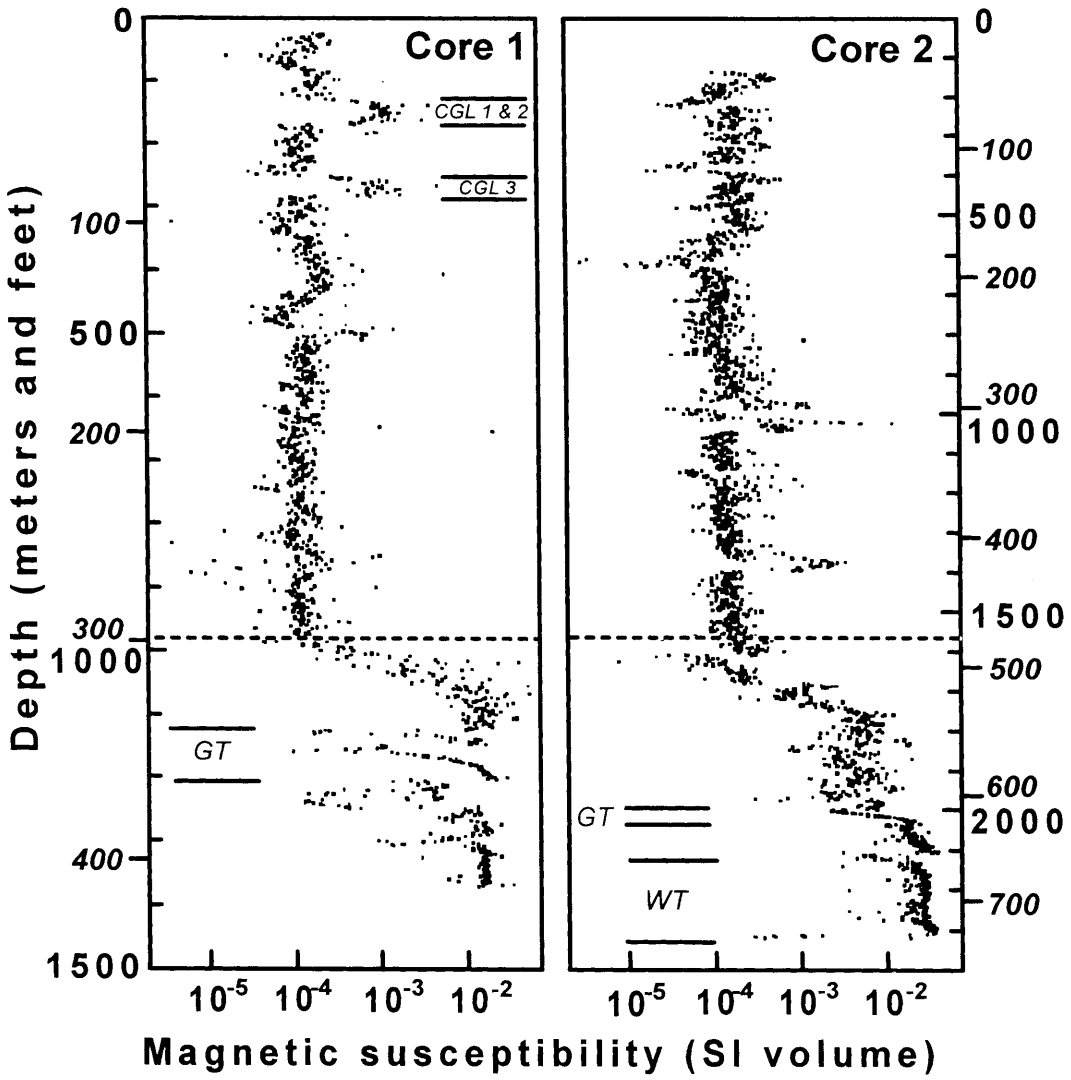

Figure 4. Magnetic susceptibility, from whole-core measurements, plotted against depth in cores 1 and 2. WT is welded tuff; GT is graded tuff; CGL is conglomerate. Dashed line approximates boundary between fluvial facies below and lacustrine facies above. Depth is shown in meters (italics) and feet.

many samples is indicated by strong increases in MS, after heating above about 400–450 °C, temperatures at which pyrite may alter to magnetite.

Petrographic observations demonstrate that sulfidization affected detrital titanium-bearing magnetite. Pyrite commonly rims magnetite (Fig. 6A) or former titanium-bearing magnetite, in which the magnetite was destroyed by complete leaching of iron (Fig. 6B). In these latter cases, the original presence of Ti-magnetite is indicated by remnants of ilmenite, or by TiO_2 formed from ilmenite, as lamellae in the {111} crystallographic orientation. Pyrite rims around former magnetite, now leached of its iron, are a common expression of sulfidization in which H_2S causes diffusion of iron from the iron oxide (Canfield and Berner, 1987; Canfield et al., 1992).

No magnetite was seen in polished sections of some samples, even though thermal demagnetization results indicated unblocking temperatures that are diagnostic for magnetite, as discussed in the following. In other polished sections, generally from coarse-grained rocks, small relicts of formerly large magnetite grains remain inside thick rims of pyrite. In some of the samples that are devoid of visible magnetite, ferrimagnetic ferrian ilmenite is present. Ferrian ilmenite was identified in polished grain mounts of magnetic-mineral separates and by thermomagnetic analysis. The resistance of ferrian ilmenite, and other varieties of the ilmenite-hematite solid-solution series, to sulfidization has been widely documented (e.g., Dimanche and Bartholomé, 1976; Reynolds, 1982; Roberts and Turner, 1993; Roberts and Pillans, 1993). These grains are optically homogeneous, with rapid cooling of the volcanic rocks having prevented exsolution into separate phases.

It is perhaps important to this study that ferrian ilmenite of a certain compositional range ($0.45 < x < 0.60$, for $Fe[III]_{2-2x}$ $Fe[II]$ Ti_x O_3) has an unusual capacity for self reversal of magnetization; i.e., the minerals may acquire a stable remanent magnetization when cooled from elevated temperatures (>~200 °C) in a direction opposite to that of the applied field (see Hoffman,

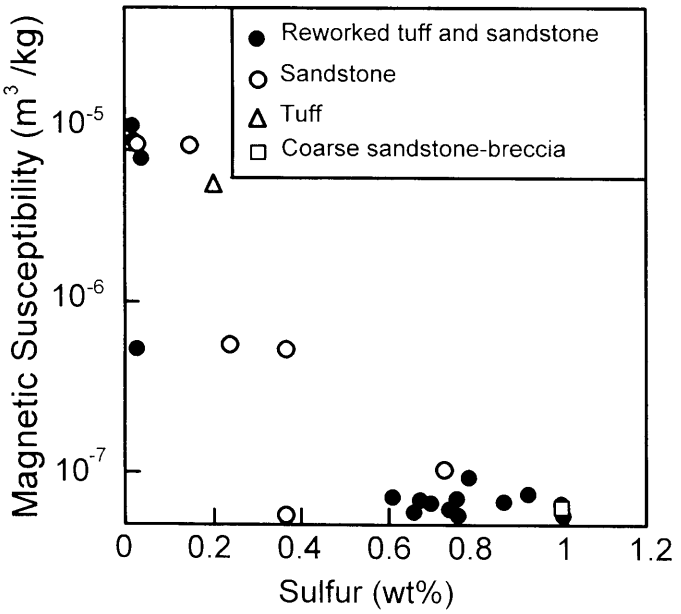

Figure 5. Plot of magnetic susceptibility against total sulfur (in weight percent) in individual samples, coded for lithic type.

1975). One thermomagnetic analysis of a magnetic extract of ferrian ilmenite (~152.4 m in core 1) gave a Curie temperature of 110 °C (Fig. 7), corresponding to a composition of $x \simeq 0.5$, which is well within the self-reversing range.

PALEOMAGNETIC RESULTS

Paleomagnetism of ash-flow tuff, core 2

Paleomagnetic behavior of the ash-flow tuff in core 2 is easily interpreted and defines a normal polarity magnetization (Fig. 8A). All 13 specimens have moderate coercivity, single-component magnetizations that together with petrographic examination imply a TRM carried by primary magnetite. The in situ mean inclination, calculated by the method of McFadden and Reid (1982), is 74.2° ($\alpha_{95} = 2.8°$). The inclination was corrected on the basis of the measured borehole attitude (azimuth 306°, offset 5° from vertical; Nelson and Kibler, 1994); the corrected mean inclination thus represents a range of possible inclinations, as illustrated in Fig. 9. The paleomagnetic results are consistent with chemical and petrographic results that confirm the basal ash-flow unit in core 2 as Snowshoe Mountain Tuff (Lipman and Weston, 1994).

Paleomagnetism of breccia and conglomerate

The tuffaceous, matrix-supported breccia in the bottom 18 m of core 1 might represent either a debris-flow deposit or a lithic-rich, nonwelded ash-flow tuff (Hulen, 1992; Larsen and Nelson, this volume). The large scatter in paleomagnetic inclinations (ranging from –35° to 80°; Reynolds et al., 1994) precludes any possibility that this unit was emplaced at temperatures to acquire a TRM or PTRM (e.g., Hoblitt and Kellogg, 1979). The scatter in remanent inclinations probably represents instead the deposition of clasts in a cold debris flow. Similarly, polymictic tuff breccia (from depths of 622–649 m and 567–594 m) as well as monomictic tuff breccia (488–549 m) in core 2 have shallow to steep, positive and negative remanent inclinations that reflect apparently random orientation of individual clasts. No consistent polarity pattern was evident when comparing nearly adjacent samples of lithic clast and matrix. These results indicate a lack of remagnetization, whether from viscous overprinting, from drilling-induced IRM, or from CRM. The abundance of unaltered, primary titano-

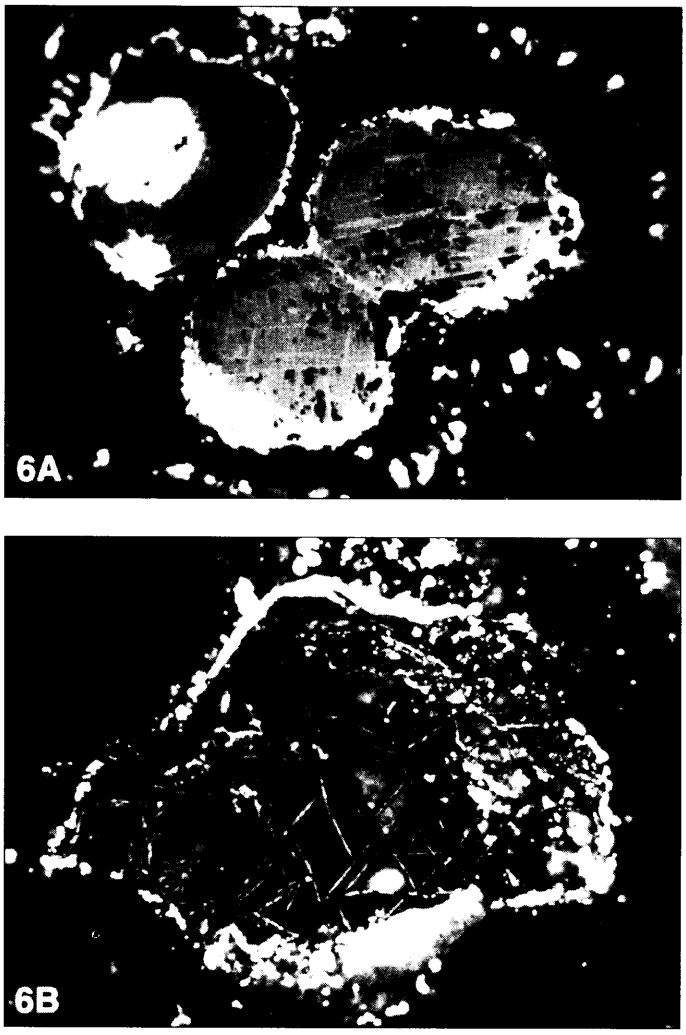

Figure 6. Reflected-light photomicrographs of polished thin section. Sample (from core 2, 71.1 m) has high natural remanent magnetization magnitude (1.3×10^{-2} A/m). A: Dumbbell-shaped titanomagnetite that is partly replaced and surrounded by pyrite (white). Magnetite (dark gray) is cut by ilmenite lamellae (light gray). Titanomagnetite grain is 140 μm in long dimension. B: Magnetite has been removed from former titanomagnetite, leaving relict ilmenite lamellae; grain is surrounded by thin rim of pyrite. Grain is 210 μm in long dimension.

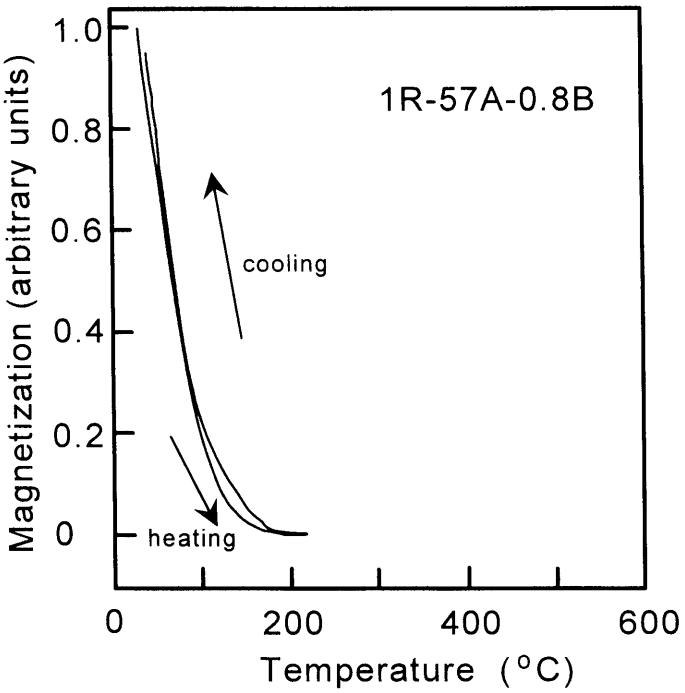

Figure 7. Thermomagnetic curve showing change in normalized magnetization as function of heating and cooling in air of magnetic separate from sandstone that contains ferrian ilmenite (sample 1R-57A-0.8B; ~152.4 m [50 ft] in core 1). Curie temperature is about 110 °C. Arrows indicate heating (down) or cooling (up) path.

magnetite in the clasts of these coarse-grained units precludes the possibility of randomizing CRM components acquired over a long time period relative to polarity reversals.

Near the top of core 1, we sampled three conglomerate units (39–51 m, 55–56 m, and 77–86 m) which we refer to informally as conglomerates 1, 2, and 3, respectively (see Reynolds et al., 1994, Fig. 2). MS is high (typically >6 × 10^{-4} volume SI), and spikes of relatively high MS near the upper and lower boundaries of conglomerate 1 (Fig. 4) resemble MS patterns related to cooling near boundaries in other volcanic rocks that may produce variations in the magnetic-mineral grain size (see Rosenbaum, 1993). The upper two conglomerates possess mixtures of positive- and negative-inclination magnetizations and thus show no evidence for the acquisition of coherent remanence, whether by TRM, PTRM, CRM, or drilling-induced IRM. In conglomerate and coarse-grained sandstone of the conglomerate-3 unit, 7 of 12 specimens possess moderate-angle (~35°–70°) positive inclinations (Fig. 8B). Of the remaining specimens, one had a shallow (18°) positive inclination, two specimens had nearly flat inclinations, and two others had negative inclinations. The predominance of specimens having positive inclinations is consistent with the acquisition of TRM or perhaps PTRM, but this possibility has not been tested using thermal demagnetization. A pervasive normal IRM can be ruled out because of the lack of uniform behavior in nearby specimens and the lack of very steep inclinations.

Paleomagnetism of ash-fall tuff and lacustrine beds

Within the lower parts of both cores, reworked, graded ash-fall tuff beds (tuff A) possess a normal polarity magnetization. Of 17 samples from the graded tuff doublet in core 1 (GT interval in Fig. 4), 16 have well-defined moderate to steep (as much as 88°) remanent inclinations (Fig. 8C and 10). The inclination trend, from steep at the bottom to shallow toward the top of each set of tuffs, suggests a drilling-induced magnetic overprint (probably a low-field IRM) on the coarse-grained tuff at the base. The simplest explanation for the sole negative inclination is that a core segment or specimen was inadvertently flipped during handling and marking. The same is not observed for the graded tuff in core 2; the average inclination calculated from the method of McFadden and Reid (1982) is 62.9° (α_{95} = 4.1°).

The ash-fall tuffs, reworked tuffs, siltstone, and sandstone in the high-sulfur, low-MS zone have predominately moderate to steep, positive or negative inclinations. No obvious polarity zonation is evident: normal and reversed polarity samples alternate through both cores 1 and 2 (Fig. 11). Many polarity changes occur over short stratigraphic intervals or within individual beds. Different polarities are found in specimens separated stratigraphically by only a few centimeters and within the same core segment. Dual polarity magnetizations are found within some individual tuff beds, each of which represents a single depositional event (Fig. 12).

The broad polarity pattern is poorly defined, and it corresponds poorly between the two cores, both in an overall sense and in detailed comparison of presumably equivalent tuffs (Fig. 11). Many samples in core 1, from tuff G down to the top of the high-MS zone, have normal polarity, whereas most samples in core 2 over this interval have reversed polarity. Furthermore, more normal than reversed polarity directions are found in tuffs E and F in core 1, but the opposite is found in these tuffs in core 2 (Fig. 11).

The polarity patterns and relations are independent of demagnetization technique. Although many fewer samples were demagnetized by thermal than by AF demagnetization, the proportion of normal and reversed polarity directions is similar after the different treatments.

Screening the results on the basis of NRM magnitude reveals a predominance of normal polarity directions (Fig. 13). Such a screen, arbitrarily accepting samples with NRM magnitudes >10^{-2} A/m, eliminates about 90% of all results from core 1 and about 80% of those from core 2, with nearly all reversed polarity directions being removed from core 1. Of the quality 1 and -2 results in core 2, only three reversed polarity directions are retained, compared to 11 normal polarity directions.

Paleomagnetism of ash-fall tuff in outcrop (site CFA-1)

The elevation of ash-fall tuff at site CFA-1 (Fig. 1) is about 2790 m, 160 m above the top of the core 2. No known struc-

tural offsets cross the essentially flat-lying Creede Formation between core 2 and site CFA-1. This tuff thus allows for a polarity determination at a horizon roughly 200 m stratigraphically above the uppermost sampled interval in drillhole 2.

The results of AF demagnetization (Fig. 14) yield a well-defined normal polarity magnetization with a mean direction of declination, D = 349.8°; inclination, I = 68.2° (α_{95} = 15.7°; k = 19.2). The normal polarity remanence is interpreted to be a DRM, because: (1) the demagnetization paths (Reynolds et al., 1994) are consistent with magnetite behavior; (2) detrital magnetite and ilmenite (probably the ferrian type) are the only magnetic minerals identified by petrographic examination; and (3) macroscopic evidence for detrimental alteration, related either to sulfidization or oxidation, is absent.

Paleomagnetism of the Fisher Dacite (postcollapse lavas of the Creede caldera)

We also measured remanent directions of lava flows from six localities (Fig. 1) of the Fisher Dacite that postdate collapse of the Creede caldera (Steven and Ratté, 1973; Steven and Lipman, 1973; Lipman, this volume). Of the six localities, only three yield straightforward paleomagnetic results with well-defined normal polarity magnetizations (Fig. 15): (1) the isotopically dated Wagon Wheel Gap lava dome (site C94-1), which erupted during sedimentation of the Creede Formation; (2) a lava flow at Mill Park that overlies this dome (C94-2); and (3) the McCall Creek flow on the west side of Snowshoe Mountain (C94-5) that erupted before caldera resurgence and then was unconformably overlain by cur-

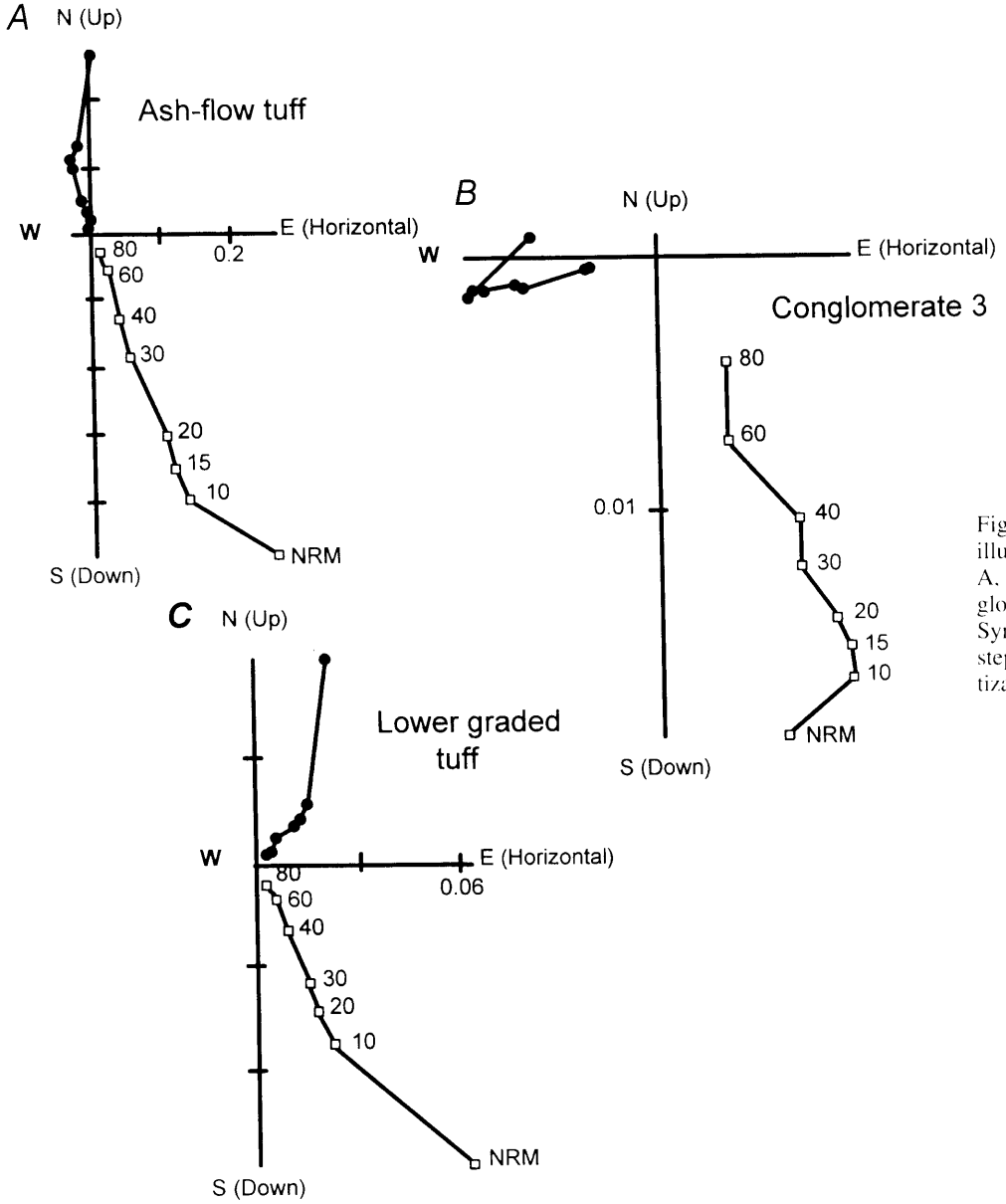

Figure 8. Orthogonal vector diagrams illustrating behavior of three lithic types: A, ash-flow tuff, core 1; B, volcanic conglomerate, core 1; C, graded tuff, core 2. Symbols as in Figure 3. (Demagnetization steps are in mT. Natural remanent magnetizations [NRM] are in A/m.)

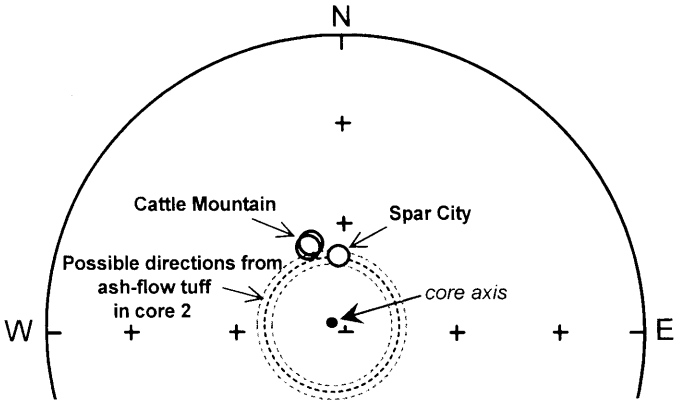

Figure 9. Equal-area projection of mean inclination of remanent magnetization from Snowshoe Mountain Tuff at bottom of core 2. Black dashed line represents possible range in azimuth of mean inclination that results from uncertainty in azimuthal orientation of the core combined with 5° offset (from vertical) in borehole attitude, as shown by orientation of core axis. Dashed lines represent uncertainty at 95% confidence level about mean inclination. Normal polarity directions of Snowshoe Mountain Tuff from outcrop sites at Cattle Mountain and Spar City are represented by 95% cones of confidence.

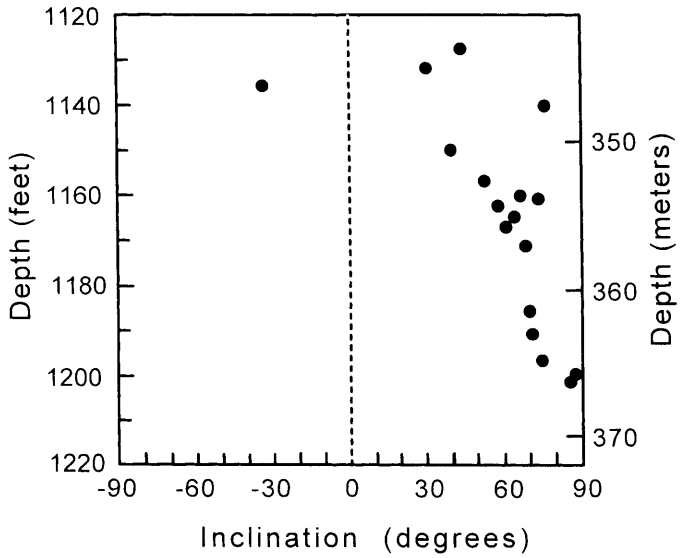

Figure 10. Plot of depth against remanent inclination for graded tuff A in core 1.

rently untilted Creede Formation beds (see Steven, 1967; Steven and Ratté, 1973; Steven and Lipman, 1973; Lipman, this volume).

Poorly exposed and isolated, blocky ledges of Fisher Dacite were also sampled on Copper Mountain at the same site from which an isotopically dated sample was obtained (Lanphere, 1994; this volume). The flow at Copper Mountain overlies Creede Formation sedimentary beds at their highest known elevation and has a $^{40}Ar/^{39}Ar$ date of 26.30 ± 0.08 Ma. The mean paleomagnetic direction, having an unusual westerly declination and relatively shallow inclination (31°), is neither clearly normal nor reversed (Fig. 15; site C94-6). Recent slumping on the mountainside, postcooling rotation off the front of a newly formed flow, or the acquisition of thermoremanence in an intermediate geomagnetic field orientation could explain this unusual direction. Two other exposures of Fisher Dacite yielded unreliable directions (Fig. 1); one was apparently affected by large-scale landsliding and the other by lightning-induced IRM.

POLARITY STRATIGRAPHY OF THE CREEDE FORMATION

Causes of apparent magnetic reversals

The most reliable paleomagnetic results reveal normal polarity magnetizations in volcanic rocks below and above the Creede Formation and intermittently in different lithologic zones within the Creede Formation. Graded tuff A in the low-sulfur, high-MS zone of the lower part of the Creede Formation has a primary normal polarity, as does the underlying Snowshoe Mountain Tuff (Fig. 11). A conglomerate bed in the upper part of core 1 has a mostly coherent normal polarity direction carried by primary titanomagnetite that is perhaps a TRM or PTRM acquired during cooling of a debris flow that was emplaced at elevated temperatures. Results from the ash-fall bed in outcrop indicate normal polarity at a horizon that is about one-third of the way up the interval between the top of core 2 and the top of the Creede Formation. Well-defined normal polarity magnetizations are found in stably magnetized lavas flows that overlie the Creede Formation.

For several reasons, the many polarity changes in the high-sulfur, low-MS zone cannot be attributed to a DRM that faithfully recorded the geomagnetic polarity at or near the time of deposition. First, many more reversals are found than can be accommodated by any geomagnetic polarity time scale over the interval between the ages of the bounding extrusive units (Figs. 2 and 11). Second, several polarity changes are recorded by specimens separated by only a few centimeters and without intervening hiatuses. Third, several individual tuff beds, each of which represents a single depositional event, contain apparent reversals. Finally, opposite polarity dominates roughly equivalent parts of the two cores—normal polarity dominates core 1 and reversed polarity dominates core 2. For reasons detailed in the following, we conclude that the complex polarity record in the lacustrine facies arises mostly from different degrees of chemical alteration and the acquisition of CRM over an extended time interval that spanned geomagnetic reversals, long after deposition of the moat-fill sediments. It is also possible that some results are from samples taken from flipped core segments.

We have tried to refine the polarity record by using magnetic characteristics to separate severely altered rocks from less altered rocks that might retain a reliable DRM. Clues to the paleomagnetic reliability of the sedimentary rocks, excluding breccia and conglomerate, are found in relations among NRM magnitude, bulk grain size, and polarity. Relatively high NRM magnitudes ($>10^{-2}$ A/m) correspond dominantly to normal polarity magneti-

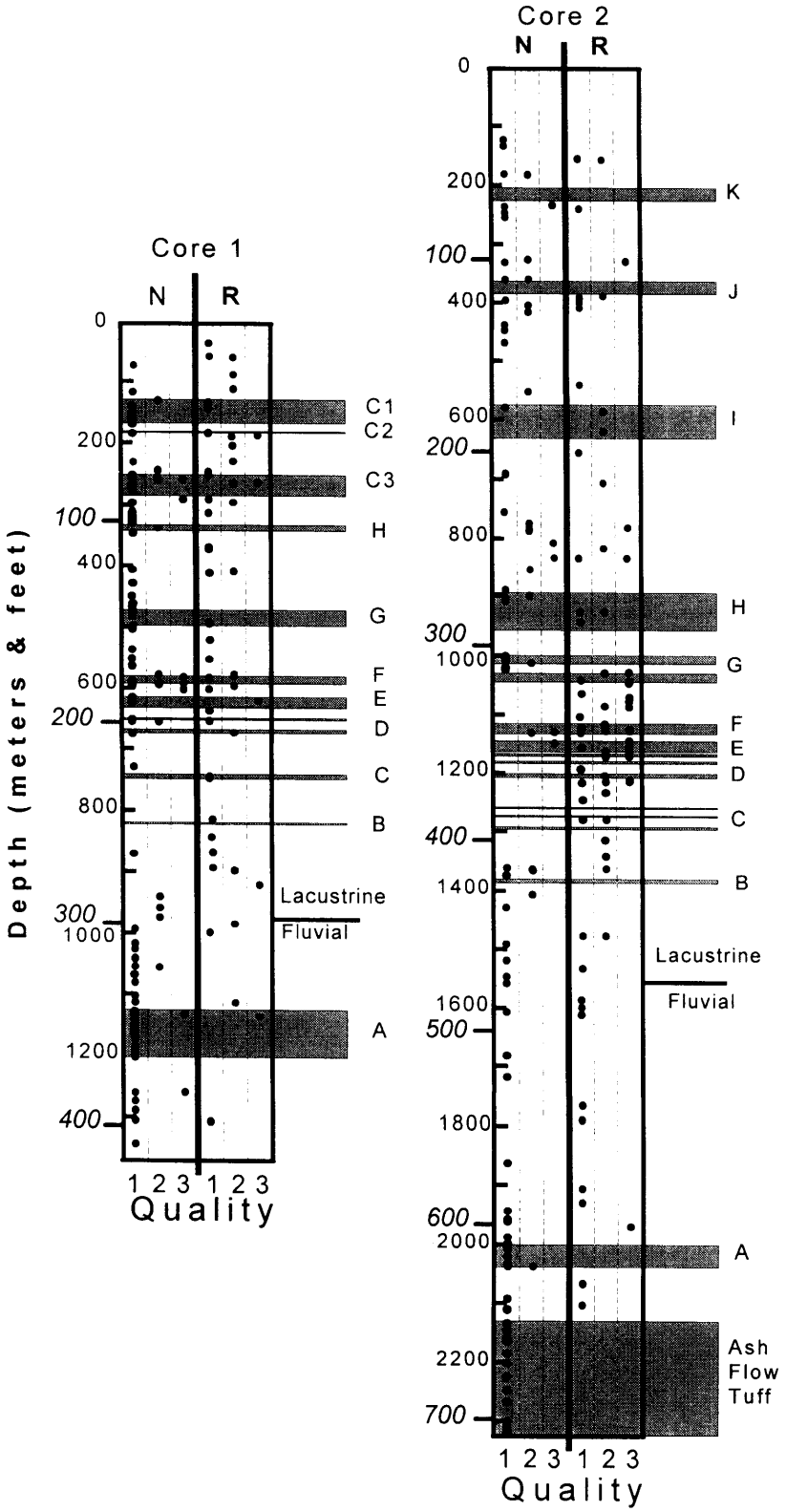

Figure 11. Summary of all paleomagnetic results from cores 1 and 2 after alternating field and thermal demagnetization. Solid circles represent normal (N) or reversed (R) polarity magnetizations, plotted in columns that represent quality of demagnetization path—1, 2, or 3 (see text). Ash-fall tuff beds are denoted by letters (A–K); C1, C2, and C3 represent conglomerates 1, 2, and 3, respectively. Depth is in meters (italics) and feet.

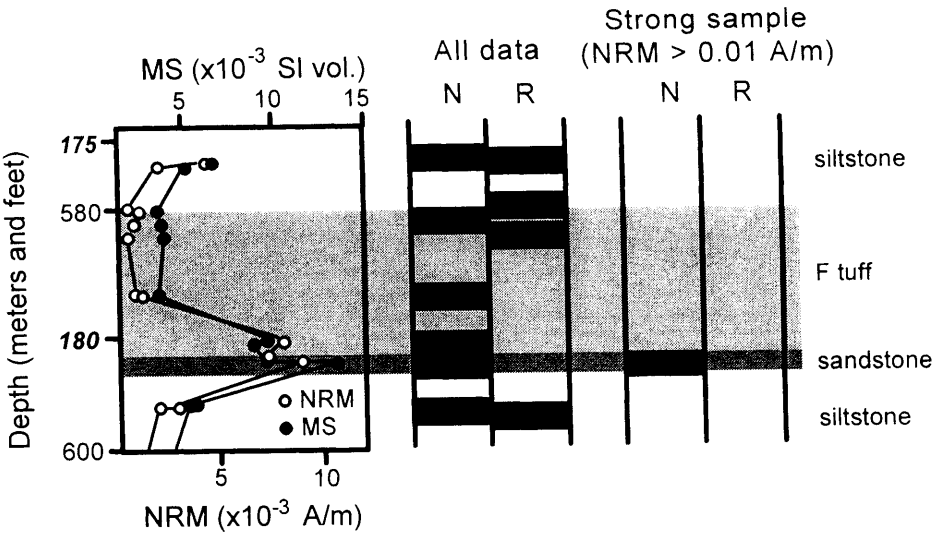

Figure 12. Variations in magnetic susceptibility (MS) and natural remanent magnetization (NRM) in tuff bed (F tuff), and in enclosing sandstone and siltstone in core 1. Changes in polarity (N, normal; R, reversed) within tuff and enclosing beds illustrate complications in establishing unambiguous polarity stratigraphy. Depth is in meters (italics) and feet.

zations (Reynolds et al., 1994, Table 1). Nearly all specimens having high-magnitude NRMs from the low-MS zone have relatively large bulk sediment grain size, typically larger than fine sand (Reynolds et al., 1994, Table 1). An example of these relations includes an ash-fall tuff bed and immediately underlying fine- to medium-grained sandstones (tuff G in core 1, about 144–154 m depth; Fig. 13). In this case, the underlying sandstone has a strong normal polarity magnetization. The coarse-grained lower part of the graded tuff also has normal polarity and higher NRM magnitude than does the interior part of the tuff. Samples from this interval having relatively strong magnetizations contain relict detrital magnetite. A further petrographic test that a reliable DRM was retained by detrital magnetite in relatively coarse grained beds was carried out on sandstone specimens from the upper 300 m in core 2. Eight quality 1 and 2 results in this interval have NRM magnitudes $>10^{-2}$ A/m, and of these, seven have normal polarity. Petrographic observations revealed detrital Fe-Ti oxide minerals in each specimen and abundant relict magnetite in some specimens.

These observations suggest that detrital magnetite in coarser grained rocks was more likely to have survived sulfidization than in fine-grained rocks. Coarse-grained beds consequently are more likely to yield a reliable polarity record. This observation is paradoxical, because fine-grained sediments, in the absence of alteration, typically give more reliable paleomagnetic results than coarse-grained sediments. A combination of small particles and the generally quiet-water environment that characterize mudstones, for example, is more conducive to efficient magnetic alignment than is the case for larger grains that are found in sandstones that may have been deposited in high-energy environments. In the highly altered Creede Formation, however, we suggest that small detrital magnetite grains in fine-grained rocks were completely removed, or nearly so, by sulfidization. Very small concentrations of secondary magnetic minerals probably account for the measurable, but weak, CRM magnetizations. In contrast, many large magnetite grains in the coarse-grained rocks had sufficient volume to withstand complete dissolution. Their initial alignment in the geomagnetic field may have been inefficient because of their size, but it was presumably was efficient enough to record the polarity in many samples. The suggestion that some sandstone in the Creede Formation adequately recorded a DRM polarity raises the problem of drilling induced remagnetization via IRM. In many sandstone samples, such IRM is expressed as a very strong and steep positive inclination NRM direction. Nevertheless, pervasive drilling-induced remagnetization to explain the dominance of normal polarity magnetizations is unlikely because (1) nearly all breccia and conglomerate beds, which contain relatively coarse grained magnetite, are randomly magnetized; and (2) most normal polarity directions stabilize after low AF demagnetization with moderate inclinations in the range of 40°–70°, reasonable values for the expected Oligocene inclination (about 56°) at the sampling latitude (Reynolds et al., 1994).

The role of ferrimagnetic ferrian ilmenite, with compositions in the self-reversing range, is uncertain as a cause for some apparent reversals. Like magnetite but with a smaller magnetic moment, it could align as an individual particle in the ambient field direction and record a DRM. There is one combination of depositional and chemical factors and events, however, that could have led to a magnetization carried by detrital ferrian ilmenite opposite to that of the geomagnetic field at the time of deposition: (1) ferrian ilmenite occurred in small (sand size or smaller) igneous rock fragments along with dominant magnetite; (2) the original TRM directions of the magnetite and ferrian ilmenite were opposite; (3) the fragments were aligned along the magnetic field direction upon deposition according to the magnetization of the magnetite; and, (4) sulfidization removed all the magnetite, leaving a remanence carried by ferrian ilmenite in the direction opposite to the applied field direction at the time of deposition. In magnetic mineral separates, we have observed rock clasts that contain ilmenite, presumably the ferrimagnetic variety, and

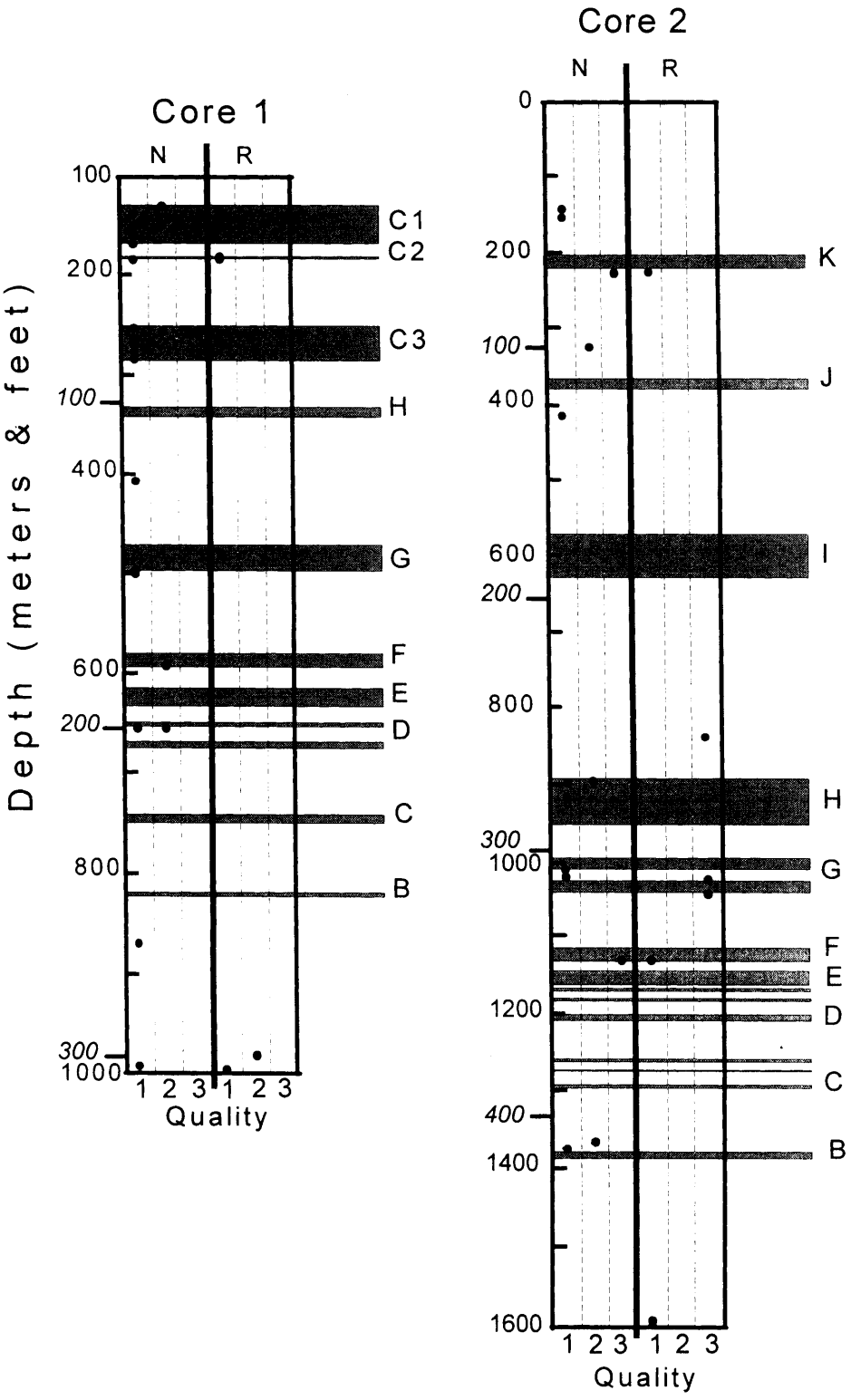

Figure 13. Summary of paleomagnetic results from cores 1 and 2 for strongly magnetized (natural remanent magnetization magnitude $>10^{-2}$ A/m) specimens after alternating field and thermal demagnetization. Solid circles represent normal (N) or reversed (R) polarity, plotted in columns that represent quality of demagnetization path—1, 2, or 3 (see text). Letter symbols as in Figure 11. Depth is in meters (italics) and feet.

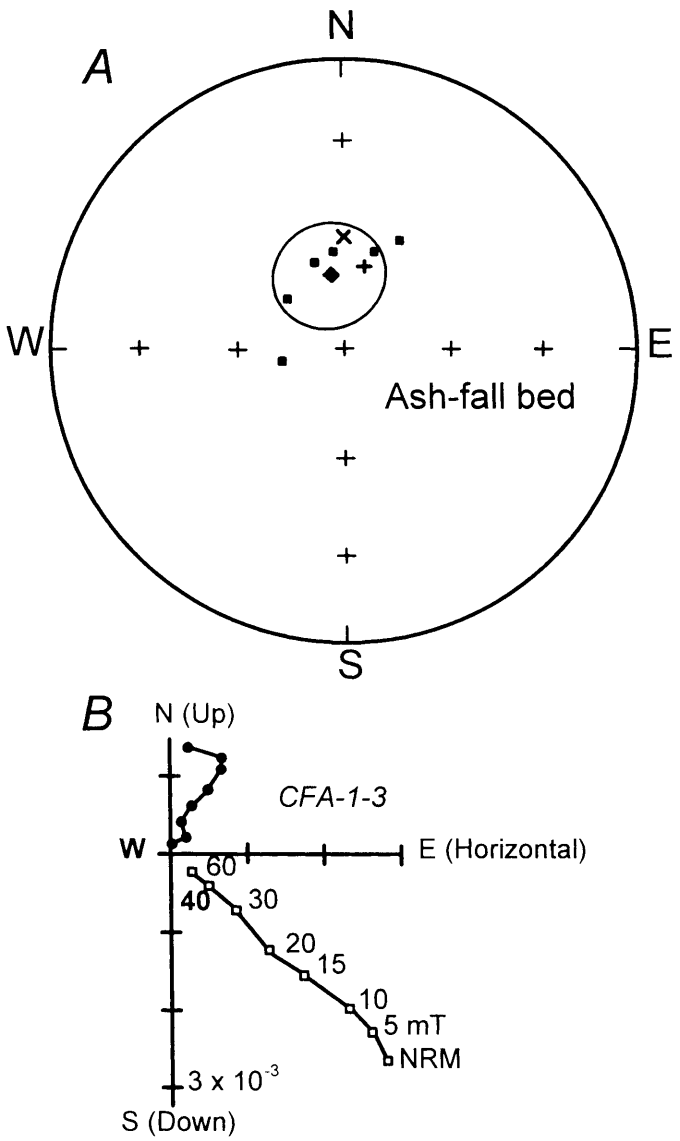

Figure 14. A: Equal-area projection of remanent magnetization directions for specimens from ash-fall tuff at site CFA-1 after alternating field demagnetization (solid squares). Mean direction (solid diamond) is surrounded by 95% cone of confidence; x is expected modern dipole field direction; + is present field direction. B: Orthogonal vector diagram of AF demagnetization behavior (steps in mT, divisions are in A/m). Symbols as in Figure 3.

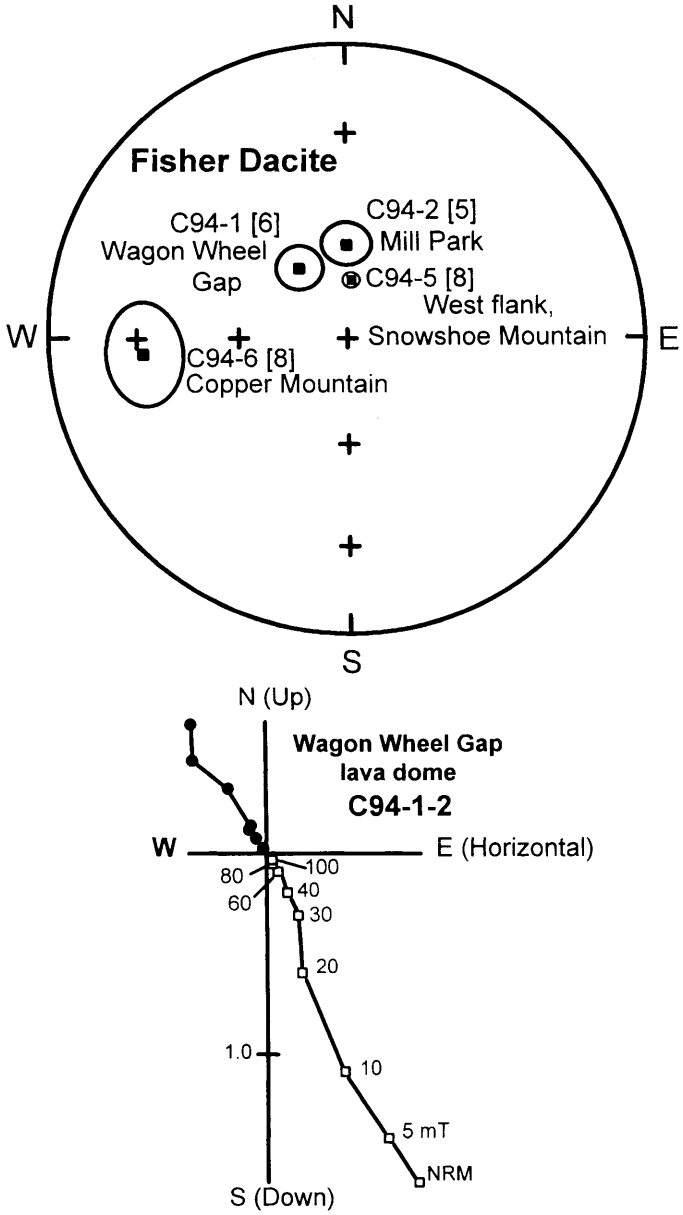

Figure 15. A: Equal-area projection of remanent magnetization directions surrounded by 95% cones of confidence for sites from postcaldera lava flows of Fisher Dacite. Number in brackets after site designation is number of specimens used in calculation of site mean. B: Representative orthogonal vector diagram showing alternating field demagnetization behavior (steps in mT) of specimen from site C94-1. Division is in A/m. Symbols as in Figure 3.

grains of altered titanomagnetite in which all magnetite relicts apparently have been removed. This scenario is thus plausible on the basis of available petrographic and thermomagnetic analyses.

The origin of the inferred secondary magnetite or maghemite that is responsible for the interpreted CRM in the low-MS zone is uncertain. The presence of magnetic iron sulfide minerals, pyrrhotite and greigite, has not been suggested by thermal demagnetization results or by thermomagnetic and petrographic analysis of magnetic and chemical separates. Hematite is similarly precluded as a widespread carrier of CRM. The incipient oxidation of pyrite may have produced secondary iron oxides. Petrographic examination of some samples indicated the presence of small regions (generally <4 μm in any dimension) in which pyrite has been replaced by a grayish iron oxide. These areas are too small to confirm the presence of magnetite or maghemite by optical properties, but are large enough to discount the presence of hematite. Such iron oxide might be responsible for the inferred CRM.

Hysteresis measurements were made on nine specimens, which were selected on the basis of polarity and strength of magnetization, in an attempt to characterize the domain states of the magnetic minerals. It was thought that fine-grained minerals, perhaps CRM-carrying iron oxides converted from pyrite and having relatively few magnetic domains, would be distinct from larger, perhaps multidomain, detrital particles. Hysteresis ratios (Fig. 16) from weakly magnetized samples (both normal and reversed polarity) are in the middle of the pseudosingle-domain field, whereas the strongly magnetized samples (all normal polarity) are closer to, or almost in, the multidomain field. This distinction, however, does not confirm the possibility that the weakly magnetized rocks are dominated by CRM components. The poor knowledge of hysteresis properties for all potentially important minerals, such as detrital ferrian ilmenite, prevents a complete interpretation. Nevertheless, the results are consistent with weak CRM carried by small pseudosingle-domain sizes relative to detrital magnetite that carries a normal DRM.

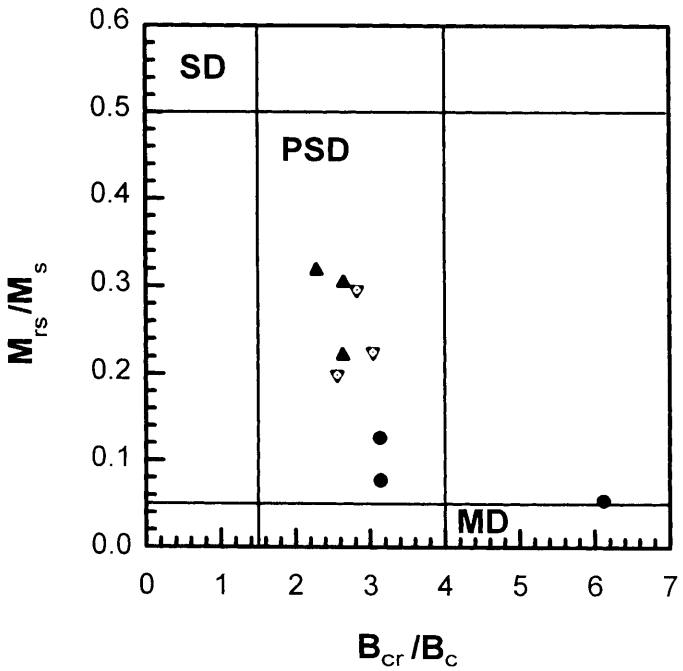

Figure 16. Plot of hysteresis ratios (see Day et al., 1977). Solid triangles denote weak-magnetization, normal polarity samples; inverted, open triangles denote weak-magnetization, reversed polarity samples; solid circles denote strong-magnetization, normal polarity samples. M_{rs}, saturation remanent magnetization; M_s saturation magnetization; B_{cr}, coercivity of remanence; B_c, coercive force. Magnetic domain areas: SD, single domain; PSD, pseudosingle domain; MD, multidomain.

Comparison of paleomagnetic results from the Creede Formation to the geomagnetic polarity time scale

The few reliable paleomagnetic results from the Creede Formation are of normal polarity. The normal polarity magnetization from graded tuff A in the lower parts of both cores and from the ashfall tuff bed in outcrop in the upper part of the Creede Formation provide the most reliable polarity data obtained. Most results from strongly magnetized samples from the lacustrine facies also indicate a normal polarity carried by detrital magnetite that has survived extensive sulfidization. The normal polarity magnetizations of the Snowshoe Mountain Tuff and of the few sites in the Fisher Dacite provide additional magnetostratigraphic constraints. None of the numerous reversed directions interspersed with normal directions in the low-MS zone of extensive sulfidic alteration can be demonstrated to be a primary DRM. We conclude that the entire Creede Formation was deposited during a normal polarity chron.

Isotopic dating of the volcanic rocks that bracket the Creede Formation suggests that caldera filling occurred over an interval of no more than about 600–700 k.y. The normal polarity magnetizations of the Creede Formation and the caldera-filling extrusive units are consistent with the dating results. For each of the three GPTSs shown in Fig. 2, the longest normal polarity interval between 26 and 27 Ma is <600 k.y. duration. Considered together, the results from paleomagnetism and isotopic dating allow the possibility that sedimentation in the Creede caldera moat occurred over an interval as short as about 300 k.y.

These combined paleomagnetic and geochronologic results can be used to refine the GPTS (Fig. 2). The interval between about 26.9 and 26.6 Ma (the ages of the Snowshoe Mountain Tuff and the Fisher flow at Wagon Wheel Gap) must be an interval of normal polarity. This conclusion is strengthened by results of other ash-flow tuffs of the central San Juan volcanic field. Three such tuffs (from oldest to youngest, the Rat Creek, Cebolla Creek, and Nelson Mountain tuffs), that are inferred on the basis of geologic relations to predate the Snowshoe Mountain Tuff but are analytically indistinguishable by $^{40}Ar/^{39}Ar$ dating, also have normal magnetizations (see Lipman, this volume; Rosenbaum et al., 1987). The 27.1 Ma Wason Park Tuff, an ash-flow tuff directly underlying the Rat Creek Tuff, is reversely magnetized (Tanaka and Kono, 1973; Beck et al., 1977). These results indicate a reversed to normal polarity boundary close to 27 Ma.

SUMMARY

In both Creede caldera moat cores, volcanic breccia, graded tuffs, and fluvial deposits having high magnetic susceptibility (MS; typically $>10^{-2}$ volume SI) are overlain by mostly fine-grained lacustrine beds and tuffs having generally lower MS (typically $<2.5 \times 10^{-4}$). The transition between high and low MS occurs over an interval of <30 m and corresponds more closely to a geochemical boundary than to a facies change. The geochemical boundary separates a deep zone with sparse pyrite from a shallow sulfidized zone with locally abundant pyrite. In the sulfidized zone, much of the pyrite formed at the expense of detrital magnetite.

This sulfidic alteration, combined with apparent acquisition of CRM components, has obscured the magnetic polarity stratigraphy. The measured paleomagnetic inclinations, most having moderate angles expected for the age and paleolatitude, seem to arise from the presence of both primary and secondary remanent

magnetizations. Rocks that contain detrital magnetite may have a dominant DRM, but rocks in which most or all such magnetite was destroyed may have a dominant CRM. Thermal demagnetization and studies of magnetic mineralogy suggest that the inferred CRM is carried by magnetite and/or maghemite. Such minerals may have formed via incipient oxidation of pyrite. Petrographic examination has not clearly revealed such CRM carriers, which, if they exist as postulated, must occur in very low concentrations (<0.003 wt%), based on NRM magnitude.

We have found no convincing evidence for a true polarity reversal within the Creede Formation. When compared to different geomagnetic polarity time scales, the combined results of paleomagnetism and isotopic dating of the volcanic rocks bracketing the Creede Formation suggest that sedimentation occurred over an interval of no more than about 600–700 k.y. and perhaps as few as about 300 k.y.

ACKNOWLEDGMENTS

We are grateful to Phil Bethke, Pete Lipman, Tom Steven, and Wayne Campbell for their support in many ways, to D. Larsen, D. Finklestein, D. Yager, and P. Nelson for useful discussions, and to M. Hudson, S. Harlan, and D. Yager for excellent technical reviews of this article. We appreciate the outstanding technical assistance of F. Gay, J. Hulen, D. Hayba, A. Hopkins, R. Streufert, W. Rivers, J. Kahn, and P. Fitzmaurice. We also gratefully acknowledge the use of the vibrating sample magnetometer at the Institute for Rock Magnetism, which is funded by the W.M. Keck Foundation, the National Science Foundation (NSF), and the University of Minnesota. This work was supported by the U.S. Geological Survey and NSF grant EAR-91-15962 (to Verosub).

REFERENCES CITED

Beck, M. E., Sheriff, S. D., and Diehl, J. F., 1977, Further paleomagnetic results for the San Juan volcanic field of southern Colorado: Earth and Planetary Science Letters, v. 37, p. 124–130.

Bethke, P. M., 1994, Research drilling in the moat of the Creede caldera, San Juan Mountains, SW Colorado, USA: Preliminary scientific results: Proceedings of the VIIth International Symposium on the Observation of the Continental Crust Through Drilling, Santa Fe, New Mexico, April 25–30, p. 9.

Bethke, P. M., and Lipman, P. W., 1987, Deep environment of volcanogenic epithermal mineralization: Eos (Transactions, American Geophysical Union), v. 68, p. 177, 187–189.

Campbell, W. R., 1993, Research drilling into the "fluid reservoir" of the Creede epithermal vein system, San Juan Mountain, Colorado, a preliminary report: Society of Economic Geologists Newsletter, April 1993, no. 13, p. 1, 3, 13–16.

Cande, S. C., and Kent, D. V., 1995, Revised age calibration of the geomagnetic polarity timescale for the Late Cretaceous and Cenozoic: Journal of Geophysical Research, v. 100, p. 6093–6095.

Canfield, D. E., and Berner, R. A., 1987, Dissolution and pyritization of magnetite in anoxic marine sediments: Geochimica et Cosmochimica Acta, v. 51, p. 645–659.

Canfield, D. E., Raiswell, R., and Bottrell, S., 1992, The reactivity of sedimentary iron minerals toward sulfide: American Journal of Science, v. 292, p. 659–683.

Dalrymple, G. B., and Lanphere, M. A., 1971, $^{40}Ar/^{39}Ar$ techniques of K-Ar dating: A comparison with the conventional technique: Earth and Planetary Science Letters, v. 12, p. 300–308.

Dalrymple, G. B., and Lanphere, M. A., 1974, $^{40}Ar/^{39}Ar$ age spectra of some undisturbed terrestrial samples: Geochimica et Cosmochimica Acta, v. 38, p. 715–738.

Dalrymple, G. B., Alexander, E. C., Jr., Lanphere, M. A., and Kraker, G. P., 1981, Irradiation of samples for $^{40}Ar/^{39}Ar$ dating using the Geological Survey TRIGA reactor: U.S. Geological Survey Professional Paper 1176, 56 p.

Day, R., Fuller, M., and Schmidt, V. A., 1977, Hysteresis properties of titanomagnetites: Grain-size and compositional dependence: Physics of Earth and Planetary Interiors, v. 13, p. 260–267.

Dimanche, F., and Bartholomé, P., 1976, The alteration of ilmenite in sediments: Minerals Science and Engineering, v. 8, p. 187–201.

Harland, W. B., Armstrong, R. L., Cox, A. V., Craig, L. E., Smith, A. G., and Smith, D. G., 1990, A geologic time scale 1989: Cambridge, Cambridge University Press, 263 p.

Hoblitt, R. P., and Kellogg, K. S., 1979, Emplacement temperature of unsorted and unstratified deposits of volcanic rock debris as determined by paleomagnetic techniques: Geological Society of America Bulletin, v. 90, p. 633–644.

Hoffman, K. A., 1975, Cation diffusion and self-reversal of thermoremanent magnetization in the ilmenite-hematite solid-solution series: Royal Astronomical Society Geophysical Journal, v. 41, p. 65–80.

Hounslow, M. W., Maher, B. A., and Thistlewood, L., 1995, Magnetic mineralogy of sandstones from the Lunde Formation (Late Triassic), northern North Sea: Origin of the palaeomagnetic signal, *in* Turner, P., and Turner, A., eds., Palaeomagnetic applications in hydrocarbon exploration and production: Geological Society [London] Special Publication 98, p. 119–147.

Hulen, J. B., 1992, Field geologic log summaries (1 in. = 12 ft.) for coreholes CCM-2 (airport 1-6) and CCM-1 (Hosselkus 1-10): University of Utah Research Institute, DOE/ER/14207-1, ESL-92001-TR, 40 p.

Jacobs, J. A., 1994, Reversals of the Earth's magnetic field: New York, Cambridge University Press, 230 p.

Kirschvink, J. L., 1980, The least-squares line and the analysis of palaeomagnetic data: Royal Astronomical Society Geophysical Journal, v. 62, p. 699–718.

Lanphere, M. A., 1988, High-resolution $^{40}Ar/^{39}Ar$ chronology of Oligocene volcanic rocks, San Juan Mountains, Colorado: Geochimica et Cosmochimica Acta, v. 52, p. 1425–1434.

Lanphere, M. A., 1994, Duration of sedimentation of the Creede Formation: U.S. Geological Survey Open-File Report 94-260C, 4 p.

Larsen, D., and Crossey, L., 1996, Depositional environments and paleolimnology of an ancient caldera lake: Oligocene Creede Formation, Colorado: Geological Society of America Bulletin, v. 108, p. 526–544.

Lipman, P. W., and Weston, P. E., 1994, Phenocryst compositions of late ash-flow tuffs from the central San Juan caldera cluster—results from Creede drillhole samples and implications for regional stratigraphy: U.S. Geological Survey Open-File Report 94-260B, 46 p.

Lipman, P. W., Sawyer, D. A., and Hon, K., 1989, Central San Juan cluster: New Mexico Bureau of Mines and Mineral Resources Memoir 46, p. 303–380.

McFadden, P. L., and Reid, A. B., 1982, Analysis of palaeomagnetic inclination data: Royal Astronomical Society Geophysical Journal, v. 69, p. 307–319.

McKibben, M. A., Eldridge, C. S., Bethke, P. M., and Rye, R. O., 1993, SHRIMP study of extreme bacteriogenic sulfur isotope enrichments in the moat sediments of the Creede caldera: Geological Society of America Abstracts with Programs, v. 25, no. 6, p. A-316.

Nelson, P. H., and Kibler, J. E., 1994, Geophysical logging and log processing, boreholes CCM-1 and CCM-2, Creede, Colorado: U.S. Geological Survey Open-File Report 94-260P, 24 p.

Reynolds, R. L., 1982, Postdepositional alteration of titanomagnetite in a Miocene sandstone, south Texas, U.S.A.: Earth and Planetary Science Letters, v. 61, p. 381–391.

Reynolds, R. L., Rosenbaum, J. G., Sweetkind, D. S., Lanphere, M. A., Rice, C. A., and Tuttle, M. L., 1994, Rock magnetic studies of the Oligocene

Creede Formation and prospects for a polarity stratigraphy: U.S. Geological Survey Open-File Report 94-260M, 44 p.

Roberts, A. P., and Pillans, B. J., 1993, Rock magnetism of Middle/Lower Pleistocene marine sediments, Wanganui Basin, New Zealand: Geophysical Research Letters, v. 20, p. 839–842.

Roberts, A. P., and Turner, G. M., 1993, Diagenetic formation of ferrimagnetic iron sulphide minerals in rapidly deposited marine sediments, New Zealand: Earth and Planetary Science Letters, v. 115, p. 257–273.

Rosenbaum, J. G., 1993, Magnetic grain-size variations through an ash-flow sheet: Influence on magnetic properties and implications for cooling history: Journal of Geophysical Research, v. 98, p. 11,715–11,727.

Rosenbaum, J. G., Reynolds, R. L., Lipman, P. W., and Sawyer, D. A., 1987, Paleomagnetism of Oligocene ash-flow tuffs, central San Juan Mountains, Colorado: Geological Society of America Abstracts with Programs, v. 19, p. 330.

Steven, T. A., 1967, Geologic map of the Bristol head quadrangle, Mineral and Hinsdale Counties, Colorado: U.S. Geological Survey Geologic Quadrangle map GQ-631, scale 1:62 500.

Steven, T. A., and Ratté, J. C., 1973, Geologic map of the Creede quadrangle, Mineral and Saguache Counties, Colorado: U.S. Geological Survey Geologic Quadrangle map GQ-1053, scale 1:62 500.

Steven, T. A., and Lipman, P. W., 1973, Geologic map of the Spar City quadrangle, Mineral County, Colorado: U.S. Geological Survey Geologic Quadrangle map GQ-1052, scale 1:62 500.

Tanaka, H., and Kono, M., 1973, Paleomagnetism of the San Juan volcanic field, Colorado, U.S.A.: Rock Magnetism and Paleogeophysics, v. 1, p. 71–76.

Wei, W., 1995, Revised age calibration points for the geomagnetic polarity time scale: Geophysical Research Letters, v. 22, p. 957–960.

Zijderveld, J. D. A., 1967, A.C. demagnetization of rocks: Analysis of results, *in* Collinson, D. W., Creer, K. M., and Runcorn, S. K., eds., Methods in palaeomagnetism: Amsterdam, Elsevier, p. 254–286.

Manuscript Accepted by the Society September 8, 1999

Printed in U.S.A.